An Investigation of Two-Dimensional Arrays of Thiolized Pd Nanocrystals

ARTICLE *in* THE JOURNAL OF PHYSICAL CHEMISTRY B · AUGUST 2000

Impact Factor: 3.3 · DOI: 10.1021/jp001242o

3 AUTHORS, INCLUDING:

P. John Thomas
Bangor University
57 PUBLICATIONS **1,624** CITATIONS
SEE PROFILE

Giridhar U Kulkarni
Centre for Nano and Soft Matter Sciences
271 PUBLICATIONS **4,436** CITATIONS
SEE PROFILE

An Investigation of Two-Dimensional Arrays of Thiolized Pd Nanocrystals

P. John Thomas, G. U. Kulkarni, and C. N. R. Rao*

Chemistry and Physics of Materials Unit, Jawaharlal Nehru Center for Advanced Scientific Research, Jakkur P.O., Bangalore 560 064, India

Received: March 31, 2000; In Final Form: June 13, 2000

Two-dimensional arrays of Pd nanocrystals of varying diameters (1.8−6.0 nm) have been obtained after thiolization with alkane thiols of different chain lengths (C_4−C_{16}). The stability and structure of these arrays have been explained in terms of the ratio of the particle diameter (*d*) and the alkane chain length (*l*). The experimental *d*−*l* phase diagram finds support from model calculations, which treat the thiolized nanocrystals as soft spheres. Generally, a *d*/*l* value between 1.5 and 3.8 gives crystalline arrays extended over several microns. For *d*/*l* values smaller than 1.5 and greater than 4.0, the nanocrystal arrays are disordered or form low-order structures.

Introduction

Metal nanocrystals in mesoscopic organizations are attracting considerable attention because of their fascinating properties and potential applications in future technology. An added dimension to this area of research is the size-dependent properties of the metal nanocrystals themselves owing to quantum confinement of the electronic states.[1] Synthesis and programmed assembly of nanocrystals of choice, therefore, assume great significance. Efforts in this direction have met with reasonable success in recent years.[2,3] In particular, metal nanocrystals coated with thiols, silanes, phospholipids, or phosphines have been shown to organize spontaneously into primitive superstructures upon drying the respective sols on flat substrates. Ohara et al.[4] reported the formation of opals from polydisperse Au nanocrystals. Low-dimensional organizations of nanocrystals in the form of dimers and trimers have been made under controlled conditions starting with Au particles coated with DNA.[5] Of special interest to us are the two-dimensional arrays of thiolized metal nanocrystals. Several workers have reported honeycomb-like organizations of Au, Ag, and Co nanocrystals.[6−8] Sarathy et al.[9] carried out thiolization of Au, Ag, and Pt nanocrystals in the size range 1−10 nm and obtained two-dimensional crystalline superlattices. Using the Langmuir−Blodgett (LB) method, Heath et al.[10] organized Ag nanocrystals into ordered assemblies at the air/water interface. A cross-linked network of Au nanocrystals[11] as well as strings consisting of large numbers of thiolized Ag nanocrystals[12] have also been obtained by the LB method.

Ligated metal nanocrystals in close-packed arrangements are driven by entropic forces such as those in hard sphere organizations. This notion has met with some success, for instance, in explaining the bimodal ensembles of Au nanocrystals.[13] A simple hard sphere model, however, fails to account for the annular ring formation by thiolized metal nanocrystals.[14] On the basis of a study of the effect of solvent polarity on the self-assembly of ligated nanocrystals, Korgel et al.[15,16] proposed a soft sphere model taking the interparticle interaction into consideration. Accordingly, a ligated nanocrystal allows for penetration of the ligand shell up to its hard sphere limit. Heath and co-workers[17] have shown that the interaction energy could be varied continually by changing the interparticle distance over a small range in the LB trough. This study led to the observation of a reversible Mott−Hubbard metal−insulator transition in a nanocrystal ensemble wherein the Coulomb gap closes at a critical distance between the particles.

We have sought to understand the nature and stability of two-dimensional crystalline arrays of thiol-covered metal nanocrystals in terms of the particle diameter, *d*, and the chain length, *l*. It has been suggested that the *d*/*l* ratio is a relevant parameter.[3,10] The penetration of the thiol shell could be different depending on *d* and *l*, which makes the investigation even more interesting. We have studied the two-dimensional arrays formed by Pd nanocrystals of varying diameter in the range 1.8−6.0 nm, by employing alkane thiols of different chain lengths, C_4−C_{16}. The study has enabled us to obtain an experimental stability diagram in terms of *d* and *l*. We have compared the experimental results with those from empirical calculations based on a soft sphere model.

Experimental Section

Thiolized Pd nanocrystals were obtained by employing a two-step procedure. The first step involved the preparation of stable, well-characterized Pd hydrosols. For this purpose, we employed the method of Teranishi et al.[18] and prepared a series of sols with mean particle diameters ranging from 1.8 to 4.5 nm. Initially, 250 mL of a 2.0 mM stock solution of H_2PdCl_4 was prepared by adding 1.73 mL of 0.58 N HCl (1.0 mM) to 88.7 mg (0.5 mM) of $PdCl_2$ in water. Then 15 mL of the stock solution was reduced by refluxing in air for 3 h with 35 mL of a ethanol−water mixture containing poly(vinylpyrrolidone) (PVP, $M_w = 40\,000$ g mol^{-1}) in different ratios to obtain various sols. The formation of the sols was marked by a gradual change in color from orange-yellow to brown-black over a period of 5 min. The sols thus obtained were examined under a JEOL-3010 transmission electron microscope (TEM) operating at 300 kV. Samples for TEM were prepared by depositing a drop of the sol on a holey carbon grid and allowing it to dry in air and then in a desiccator overnight.

The hydrosol obtained using 40% ethanol and a PVP/Pd ratio of 40 contained nanocrystals of mean diameter 1.8 nm. The

* Corresponding author. E-mail: cnrrao@jncasr.ac.in.

10.1021/jp001242o CCC: $19.00
Published on Web 07/29/2000

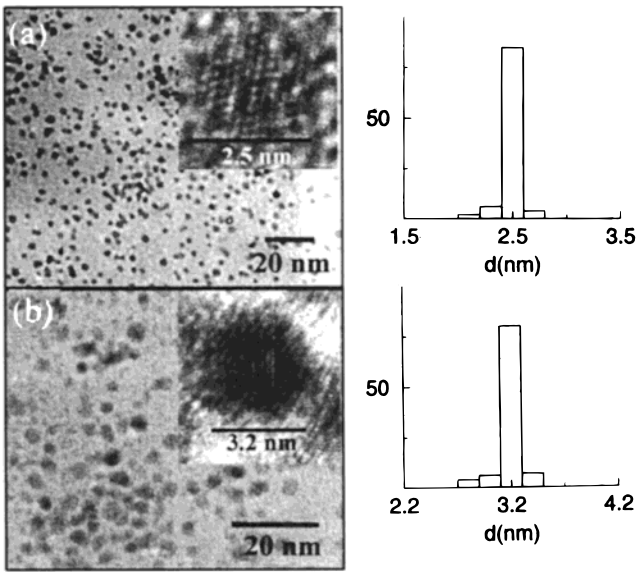

Figure 1. TEM micrographs showing PVP-covered Pd nanocrystals prepared under different reducing conditions: (a) 20% ethanol, PVP/Pd = 10, (b) 25% ethanol, PVP/Pd = 10. Histograms in the insets show the size distribution (in percentage). High-resolution images of individual particles are also shown.

size distribution as seen with TEM was quite narrow ($\sigma \sim 15\%$). Monodispersed Pd nanocrystals of diameter 2.5 nm were obtained using 20% ethanol at a PVP/Pd ratio of 10. Teranishi et al.[19] have assigned a magic nuclearity of 561 to the nanocrystals thus prepared. Although one cannot entirely be certain that the nanocrystals contained exactly 561 atoms in the five-shell closed configuration, the particles were monodispersed with a uniform diameter of 2.5 nm ($\sigma \sim 6\%$), as evidenced by TEM (Figure 1a) and as expected of a nuclearity of 561. High-resolution imaging showed the icosahedral shape of the particles and confirmed their crystalline nature (see inset in Figure 1a). Seven-shelled Pd_{1415} nanocrystals (diameter $\sim$ 3.2 nm, $\sigma \sim 7\%$) were prepared by changing the ethanol−water composition to 25%. An HRTEM image of an individual nanocrystal showed 15 [111] fringes corresponding to a Pd_{1415} particle[20] (Figure 1b). A Pd sol containing bigger particles was obtained by a growth process starting with the 2.5 nm (Pd_{561}) sol. Equal volumes of as-prepared Pd_{561} sol and 0.6 mM H_2PdCl_4 in ethanol−water (2:3) were refluxed for 1 h, which yielded particles of $\sim$4.5 nm diameter. Yet another Pd sol was prepared by reducing 33.5 mg of $Pd(OAc)_2$ with ethanol (125 mL) in the presence of 190 mg of PVP.[21] A mean particle diameter of $\sim$6.0 nm was obtained in this case. The size distribution in the last two sols was slightly broader ($\sigma \sim 14\%$) compared to the extremely narrow distributions of the 2.5 nm and the 3.2 nm sols.

The hydrosols were subjected to thiol-derivatization by the method described by us recently.[9] Thus, to 3 mL of a 0.6 mM Pd sol were added 0.4 mL of toluene and 10 μL of an alkanethiol. The two layers were thoroughly mixed with a vortex mixer. To this was added 3 mL of concentrated HCl over a period of 3 min under vigorous stirring. This resulted in a complete transfer of color across the bilayer interface, with the aqueous layer in the bottom turning colorless. HRTEM images showed that the transfer was indeed faithful in that the size and the shape of the nanocrystals, especially the smaller ones, remained unchanged. Thiolized Pd nanocrystals were characterized by X-ray photoelectron spectroscopy (XPS). For this purpose, a ESCALAB MKIV spectrometer employing Al Kα radiation (1486.6 eV) was used. Samples for XPS measurements were prepared by depositing a few drops of the sol on an amorphized graphite substrate. The binding energy of the Pd($3d_{5/2}$) core-level was at 334 eV, corresponding to metallic Pd in both cases—before and after thiolization. However, the N(1s) feature at $\sim$400 eV present in the PVP-protected Pd nanocrystals was not seen after thiol derivatization. Instead a new feature at 163.5 eV due to S(2p) was seen, showing that the thiol molecules were chemisorbed on the surface of the Pd nanocrystal in the organosol.

Results and Discussion

In Figure 2 we show TEM micrographs obtained with nanocrystals of diameters 2.5 and 3.2 nm, derivatized using octanethiol and dodecanethiol, respectively. Organized arrays of these nanocrystals extending over several microns were seen in the images. The honeycomb-like ordering of the nanocrystals propagates a few tens of nanometers before being interrupted by a line or point defect[22] (see arrows in Figure 2). With the change of thiol from C_8 to C_{12}, the packing of nanocrystals looks somewhat different (compare parts a and c with b and d of Figure 2, respectively). The self-assembly of the thiol molecules on the faceted nanocrystal surface perhaps determines the structure of the organization.[16] The 2.5 nm particles coated with octanethiol (Figure 2a) exhibit a pattern where a nanocrystal at the center of a hexagon is more prominent compared to the surrounding ones. The 3.2 nm particles coated with dodecanethiol (Figure 2c) also organize in a similar fashion. These are essentially bilayered structures[23] where the nanocrystals in the top layer occupy 2-fold saddle sites to form a hexagon which is rotated by 30° with respect to the hexagon below. On the other hand, the hexagonal arrays shown in Figure 2b (2.5 nm/dodecanethiol) and 2c (3.2 nm/octanethiol) are more commonly observed.[6−9] A special feature of the above four arrays is that they are composed of near-magic nuclearity nanocrystals. Schmidt et al.[24] have recently reported the formation of ordered two-dimensional monolayers of Au_{55} nanocrystals on a polymer film. In the present study, however, nanocrystals of choice are thiolized and organized.

We have analyzed the two-dimensional lattices of thiolized nanocrystals in terms of the distributions in the nearest neighbor distance, c, as well as the angle, α, subtended by a pair of nearest neighbors using a computer code developed by us. The code was initially tested on a mathematically generated hexagonal lattice. It produced single line histograms corresponding to the lattice dimension and the hexagonal angle (60°), respectively. The histograms obtained with the lattices are shown in the respective insets. From the inset in Figure 2b, we get the mean values of c and α for the 2.5 nm particles coated with dodecanethiol: $c = 4.1$ nm ($\sigma = 8\%$) and $\alpha = 60°$ ($\sigma = 13\%$). Assuming the fully extended all-trans conformation of the dodecanethiol molecule inclined at 30° on the particle surface,[10] its projected chain length (l) is $\sim$1.7 nm. Accordingly, the expected c value (diameter plus twice the chain length) is $\sim$5.9 nm. The observed value of 4.1 nm is considerably smaller due to the interpenetration of the ligand shells of the neighboring nanocrystals. A reduction in the c value of 1.8 nm amounts to 53% interdigation of the thiol molecule. On the contrary, the octanethiol molecules on the 3.2 nm particles (Figure 2c) exhibit 25% interdigation ($c = 5.0$ nm, $l = 1.2$ nm). The histograms in parts a and d of Figure 2 refer to the second neighbors, and the interdigation of the thiol molecules in these cases is estimated to be 48% and 31%, respectively. From the insets in Figure 2, we observe that the distribution in the angle α is somewhat narrower in the case of dodecanethiol-assisted organizations.

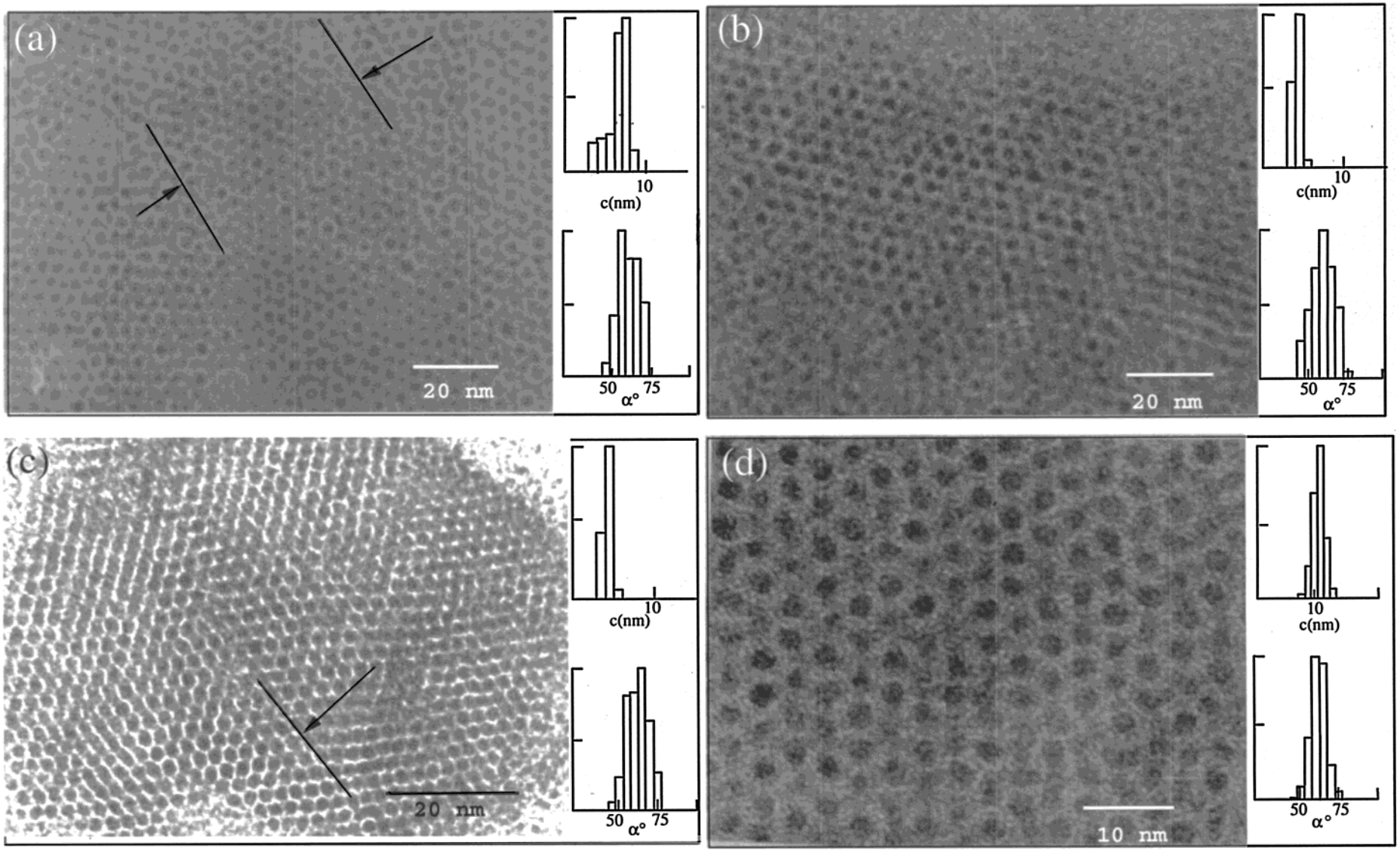

Figure 2. TEM micrographs showing hexagonal arrays of thiolized Pd nanocrystals: (a) 2.5 nm, octanethiol (b) 2.5 nm, dodecanethiol (c) 3.2 nm, octanethiol, and (d) 3.2 nm, dodecanethiol. Histograms in the insets show distributions (in percentage) in the nearest neighbor distance, *c*, and the angle, α. The arrows indicate line defects.

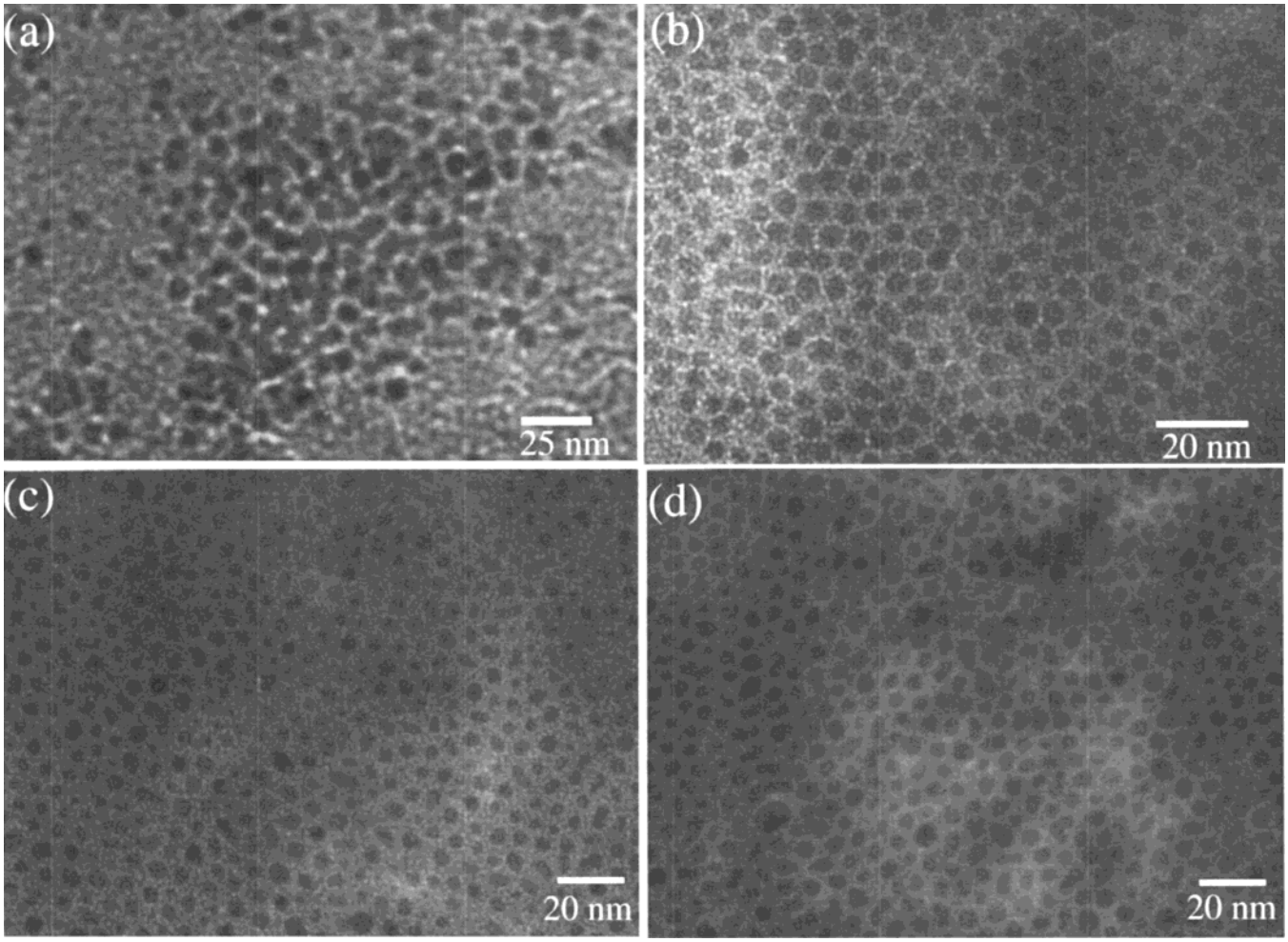

Figure 3. TEM micrographs showing Pd nanocrystals of mean diameter 4.5 nm organized into two-dimensional lattices using different thiols: (a) butanethiol, (b) octanethiol, (c) dodecanethiol, and (d) hexadecanethiol.

The effect of the thiol chain length on nanocrystal organization is illustrated in Figure 3 in the case of the 4.5 nm nanocrystals. The butanethiol-coated nanocrystals form agglomerates, 20−40 nm in size, with little internal order (Figure 3a). In many regions, the particles do not show distinct boundaries. The mean diameter estimated from the isolated particles (∼4.6 nm) is similar to that of the pristine sol. Longer chain thiols, on the other hand, give rise to close-packed arrays (Figure 3b−d) spread over micron-sized areas similar to those shown in Figure 2. The contrasting behavior of butanethiol (Figure 3a) is clearly due to its short chain length ($l = 0.8$ nm) and not related to the concentration of the sol, since similar conditions of preparation were used in all the cases. The role of the thiol chain length becomes more apparent when we closely examine the organizations in Figure 3b−d. The 4.5 nm nanocrystals covered with octanethiol form a honeycomb lattice (Figure 3b) which is relatively less dense compared to the lattices in Figure 2. We observe short-range order limited to three or four hexagons of nanocrystals. The packing is facilitated in many places by a curved arrangement of the nanocrystals. The interparticle distance, *c*, calculated from relatively dense areas is ∼6.2 nm ($\sigma \sim 11\%$), which amounts to thiol interdigation of 30%. On the other hand, the 4.5 nm sol derivatized with dodecanethiol and hexadecanethiol, crystallize in close-packed structures as shown in parts c and d, respectively, of Figure 3. The nanocrystals are, however, not uniform in size. The mean sizes are similar to the pristine sol, but the distributions have considerably widened ($\sigma \sim 20\%$ and 18%, respectively). Unlike the near-magic nuclearity particles, the 4.5 nm particles exhibit wider size distribution in the hydrosol and are more susceptible to change in size and shape after thiolization. Despite the variations in shape and size, the nanocrystals organize into close-packed arrays, as shown in Figure 3c,d. The corresponding *c* values are 7.3 nm ($\sigma^2 \sim 14\%$) and 7.7 nm ($\sigma^2 \sim 12\%$), respectively, the interpenetration of thiol molecules being ∼18% and 24%, respectively. These organizations are different from the opal structures observed by Ohara et al.[4] and resemble more closely the jammed arrangements of polydisperse spheroids.[25]

The results discussed above suffice to demonstrate that the nature of nanocrystal organization depends on both the particle diameter, *d*, and the thiol chain length, *l*. On the basis of our study of the nanocrystal organizations obtained with different values of *d* and *l*, we have arrived at the phase diagram shown in Figure 4. In this figure, the bright area in the middle is the most favorable *d*/*l* regime, corresponding to extended close-packed organizations of nanocrystals such as those illustrated in Figures 2 and 3. The *d*/*l* values in this area are in the range 1.5−3.8. The area shaded dark in Figure 4 includes the *d*/*l* regime giving rise to various short-range aggregations, formed when the particles are small and the chain length is large, or vice versa. As an example, we show a TEM image of 6 nm/octanethiol ($d/l \sim 5.0$) assembly in Figure 5 which exhibits no long-range order. However, the nanocrystals are isolated from

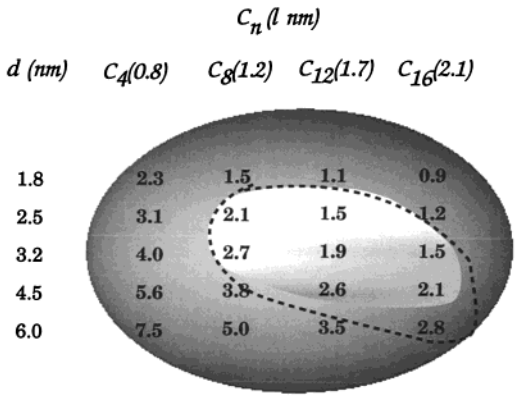

Figure 4. The $d-l$ phase diagram for Pd nanocrystals thiolized with different alkane thiols. The mean diameter, d, was obtained from the TEM measurements on as-prepared sols. The length of the thiol, l, is estimated by assuming an all-trans conformation of the alkane chain. The thiol is indicated by the number of carbon atoms, C_n. The bright area in the middle encompasses systems which form close-packed organizations of nanocrystals. The surrounding darker area includes disordered or low-order arrangements of nanocrystals. The area enclosed by the dashed line is derived from calculations from the soft sphere model.

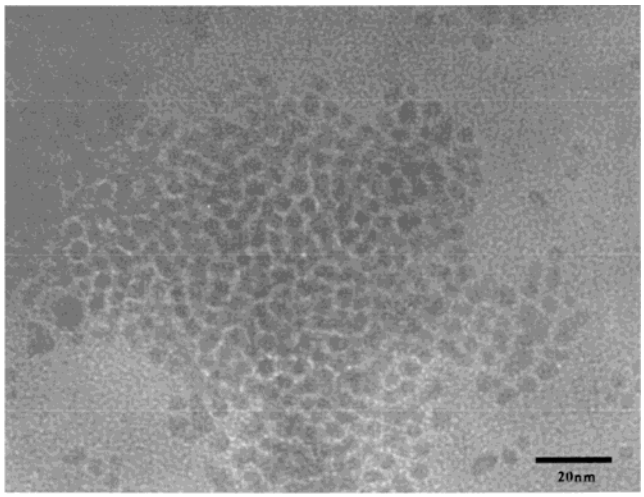

Figure 5. TEM micrograph showing disordered arrangement of 6 nm particles coated with octanethiol ($d/l \sim 5.0$).

one another, unlike those in Figure 3a. This organization resembles a collapsed monolayer of metal particles observed in the LB method upon applying pressure.[10]

To shed further light on the above experimental observations, we invoke the soft-sphere model proposed by Korgel et al.[16] In this model, the total potential energy (E) is considered to be a result of two types of forces between the nanocrystals,

$$E = E_{\text{steric}} + E_{\text{vdW}} \tag{1}$$

The van der Waals interaction due to the polarization of the metal cores constitutes the attractive term and the steric interaction between the thiol molecules on the two surfaces forms the repulsive term,

$$E_{\text{vdW}} = \frac{A}{12}\left\{\frac{d^2}{\tau^2 - d^2} + \frac{d^2}{\tau^2} + 2\ln\left(\frac{\tau^2 - d^2}{\tau^2}\right)\right\} \tag{2}$$

$$E_{\text{steric}} = \frac{50dl^2}{(\tau - d)\pi\sigma_a^3} kT e^{-\pi(\tau - d)} \tag{3}$$

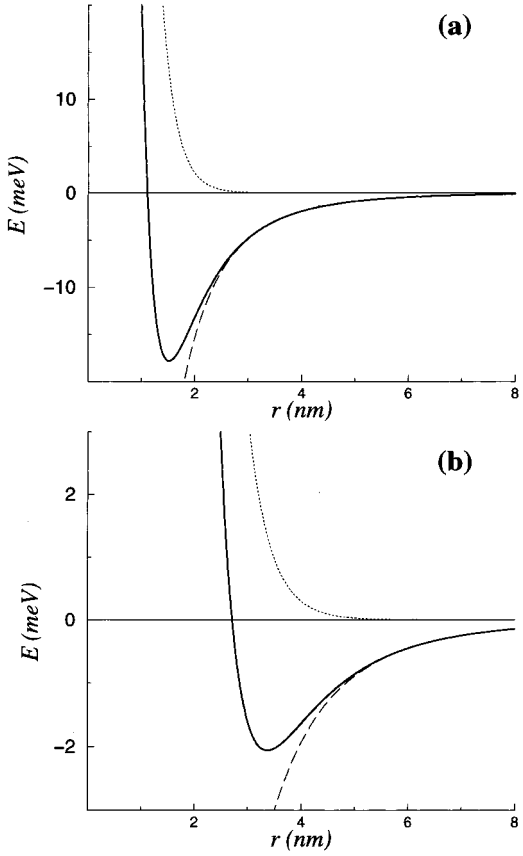

Figure 6. Variation of the two components and the total potential energy versus the separation distance between two nanocrystals of 4.5 nm diameter coated with (a) octanethiol or (b) dodecanethiol.

where τ is the interparticle distance. The Hamaker constant, A, for Pd nanocrystals in toluene has been estimated to be 1.95 eV.[26] The calculated diameter of the area occupied by the thiol molecule (σ_a) on the particle surface is ~4.3 Å.[16] The total energy is attractive over a range of interparticle distances, the magnitude increasing with fall in distance. There could be a range of interparticle distances where the attractive energy from the van der Waals term exceeds the repulsive energy due to the steric factor, giving rise to net stabilization of the two-particle system. This is illustrated in Figure 6 in the case of 4.5 nm particles. Stabilization energies of 17 and 2 meV were obtained from the calculation for particles coated with octanethiol and dodecanethiol, respectively.

In Figure 7 we depict the stabilization energies for d/l values corresponding to the experimentally investigated systems. The points fall in two regions corresponding to organized and unorganized arrays. With shorter thiol chain lengths or larger metal cores ($d/l > 3$), we observe steep potential energy wells in the range of tens of millielectronvolts, possibly implying agglomeration of the particles. For $d/l < 1.5$, the two-particle system exhibits a shallow minimum with negligible stabilization, corresponding to a situation where long thiol chains shield the attractive interactions between the metal cores. An organization of this kind is influenced more by the directional property of the thiol chain, resulting in lower order structures. For d/l values in the range ~2.0−3.0, the stabilization energies have moderate values comparable to the thermal energy of the nanocrystals (see the regime marked by the dashed line in Figure 4). This energy is just adequate to bring the metal particles close enough to form an extended array. This is similar to the case of hard spheres where the interaction energy is negligible till the spheres come in contact and the repulsion is then asymptotic.[27] Thiolized

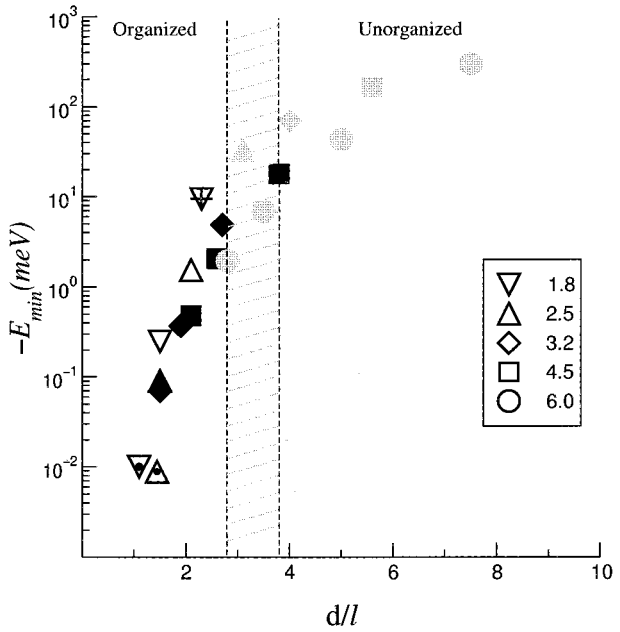

Figure 7. Variation of the stabilization energy against *d*/*l* for various nanocrystal−thiol systems: filled squares, crystalline organization; plus, dimers and trimers; centered, 1-D string; gray, disordered organization. The organized and unorganized regions are delineated with the hatched area indicating an intermediate region.

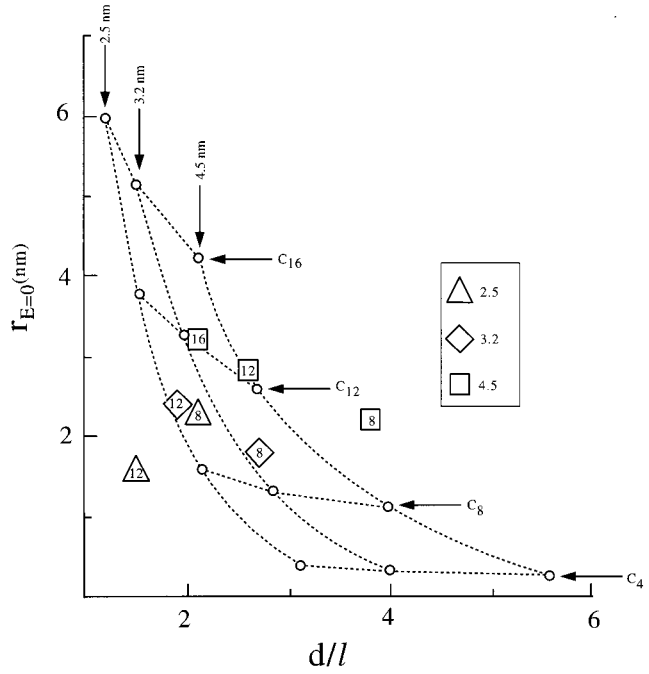

Figure 8. Separation distance at the zero crossover of the total potential ($r_{E=0}$) against *d*/*l* for various nanocrystal−thiol systems. The separation distances in close-packed organizations of nanocrystals obtained from TEM are also shown.

nanocrystals in the hard sphere limit are guided mainly by the entropy, leading to the honeycomb organization.

In Figure 8, we present the separation distances obtained in the hard sphere limit ($r_{E=0} = c_{E=0} - d$) for the different nanoparticles and thiols in the form of a grid against *d*/*l*. For a given thiol, the separation distance increases as the nanocrystal diameter decreases, more steeply when the thiol chain is longer. Compared to these results, our experimental values lie between 1.5 and 3.2 nm. It is clear from Figure 8 that our calculations underestimate the distance in the case of octanethiol, the

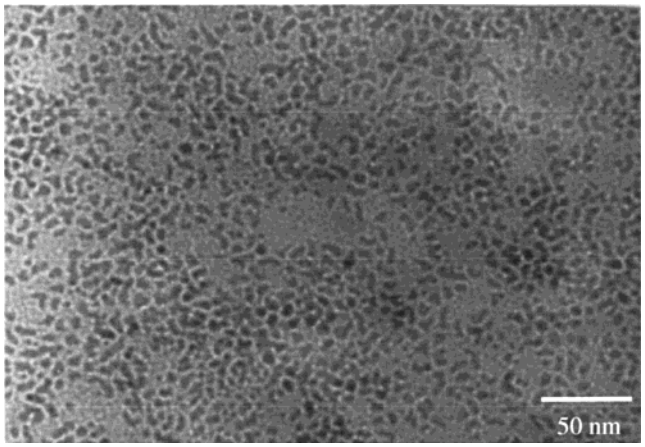

Figure 9. TEM micrograph showing aggregates of 1.8 nm particles covered with butanethiol.

deviations being 44%, 13%, and 25% for 2.5, 3.2, and 4.5 nm particles, respectively. The values are overestimated by as much as 50% for the longer thiols. In other words, the thickness of the thiol shell, l', estimated from the experimental separation distances ($2l' = c - d$) is different compared to the projected lengths (*l*). Accordingly, the ratio *d*/l' for the experimental crystalline lattices falls in the range 2.5−4.0 as compared to the *d*/*l* range of 1.5−3.8. Clearly, the extent of interdigation of thiol molecules plays a major role in attributing hardness to the ligated nanocrystal, which in turn decides the nature of the two-dimensional organization.

We now briefly examine organizations in systems where the dimensions of the metal core and of the thiol reach have extreme values, as in the case of 1.8 nm particles coated with butanethiol (Figure 9). The *d*/*l* value in this case is 2.3 and the stabilization energy is relatively high, (∼10 meV; see Figure 7). We see from Figure 9 that the nanocrystals are engaged locally in small aggregates to form dimers, trimers, or occasionally even tetramers. The aggregates mingle with one another to give rise to what could be efficient packing under the given constraints. Clearly, the butanethiol molecule, despite being attached to a small nanocrystal (1.8 nm) fails to prevent agglomeration of the metal cores. In extreme cases such as this, the *d*/*l* criterion alone would not suffice for the formation of a nanocrystal array. Another interesting arrangement is seen in the case of the 3.2 nm particles covered by hexadecanethiol (*d*/*l*, 1.5), the stabilization energy of which is very small (see Figure 7). The metal nanocrystals are not sufficiently big to attract hexagons of partners but instead form a loose structure filled with 1-D strings, as shown in Figure 10. Each string is identified with a series of nearly equally spaced ($c \sim 6.3$ nm, $\sigma^2 \sim 14\%$) nanocrystals, corresponding to 26% of interdigation of the hexadecanethiol molecules. The length of the string varies between 15 and 65 nm (3 and 12 particles, respectively) with the mean at 35 nm (6 particles). A vector sum of the strings gives a small residue (6 nm), implying that the arrangement is indeed random. This type of arrangement is observed, though less prominently, in the case of 1.8 and 2.5 nm particles covered with hexadecanethiol.

A critique of the *d*/*l* model would be in order at this stage. This model takes account of competing forces arising from the attraction between the metal cores and the steric repulsion from the surface ligands. The question as to how good *d*/*l* is as an operational parameter is debatable. As shown earlier, the *d*/*l* ratio for crystalline lattices is in the range ∼1.5−3.8, the only strong exception being the 1.8 nm/butanethiol system (*d*/*l*, 2.3)

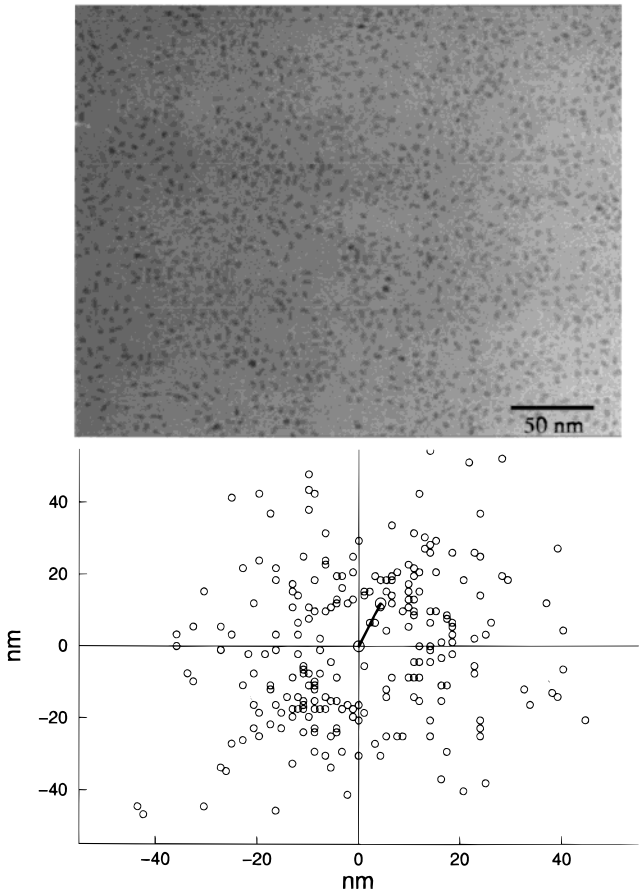

Figure 10. TEM micrograph showing 1-D strings of 3.2 nm particles held by hexadecanethiol. In the plot below are shown the vectors depicting the length and direction of the strings with the center of the picture as the origin. The resultant obtained by adding the vectors is indicated as a thick line.

which forms a low-dimensional organization. Nanocrystal systems such as 1.8 nm/dodecanethiol and 6.0 nm/butanethiol, with d/l far outside this range, exhibit disordered structures. It is, therefore, gratifying that the simple d/l model accounts for the experimental observations reasonably satisfactorily, except at the boundary values. Clearly, there is need to examine thiol interdigation and related problems associated with the nanocrystalline arrays.

Conclusions

Thiolized Pd nanocrystals self-assemble to give rise to different types of organizations depending on the particle diameter, d, and the alkane chain length l. The experimental observations relating the stability of the two-dimensional arrays to the d/l ratios find support from empirical calculations based on a soft sphere model. Nanocrystals with stabilization energies comparable to the thermal energy (a few millielectronvolts) give rise to close-packed hexagonal crystalline arrays whose d/l values are in the range 1.5−3.8. Large nanocrystals ($d/l > 3$) with high stabilization energies (>10 meV) form collapsed structures while those attached to longer chain thiols ($d/l \leq 1.5$) are associated with little stabilization and exhibit low-order structures. The interparticle distances estimated from the soft sphere model deviate to some extent from the experimental values due to the interdigation of thiol molecules chemisorbed on the curved nanocrystal surfaces.

References and Notes

(1) Edwards, P. P.; Johnston, R. L.; Rao, C. N. R. In *Metal clusters in chemistry*; Braunstein, P., Oro, G., Raithby, P. R., Eds.; Wiley-VCH: New York, 1999.

(2) Rao, C. N. R.; Kulkarni, G. U.; Thomas, P. J.; Edwards, P. P. *Chem. Soc. Rev.* **2000**, *29*, 27.

(3) Whetten, R. L.; Shafigullin, M. M.; Khoury, J. T.; Schaaf, T. G.; Vezmar, I.; Alvarez, M. M.; Wilkinson, A. *Acc. Chem. Res.* **1999**, *32*, 397.

(4) Ohara, P. C.; Leff, D. V.; Heath, J. R.; Gelbart, W. M. *Phys. Rev. Lett.* **1995**, *75*, 3466.

(5) Alivasatos, A. P.; Johnsson, K. P.; Peng, X.; Wilson, T. E.; Loweth, C. J.; Bruchez, M. P.; Schultz, P. G. *Nature* **1996**, *382*, 609.

(6) Whetten, R. L.; Khoury, J. T.; Alvarez, M. M.; Murthy, S.; Vezmar, I.; Wang, Z. L.; Stephens, P. W.; Cleveland, C. L.; Luedtke, W. D.; Landman, U. *Adv. Mater.* **1996**, *8*, 428.

(7) Harnifest, S. A.; Wang, Z. L.; Whetten, R. L.; Vezmar, I.; Avarez, M. M. *Adv. Mater.* **1997**, *9*, 817; Korgel, B. A.; Fritzmaurice, D. *Adv. Mater.* **1998**, *10*, 661.

(8) Sun, S.; Murray, C. B. *J. Appl. Phys.* **1999**, *85*, 4325. Petit, C.; Taleb, A.; Pileni, M. P. *J. Phys. Chem. B*, **1999**, *103*, 1805.

(9) Sarathy, K. V.; Kulkarni, G. U.; Rao, C. N. R. *Chem. Commun.* **1997**, 573. Sarathy, K. V.; Raina, G.; Yadav, R. T.; Kulkarni, G. U.; Rao, C. N. R. *J. Phys. Chem. B* **1997**, *101*, 9876.

(10) Heath, J. R.; Knobler, M. C.; Leff, D. V. *J. Phys. Chem. B* **1997**, *101*, 189.

(11) Chen, S. *Adv. Mater.* **2000**, *12*, 186.

(12) Chung, S. W.; Markovich, G.; Heath, J. R. *J. Phys. Chem. B* **1998**, *102*, 6685.

(13) Kiely, C. J.; Fink, J.; Brust, M.; Bethell, D.; Schiffrin, D. J. *Nature* **1998**, *396*, 444.

(14) Ohara, P. C.; Heath, J. R.; Gelbart, W. G. *Angew. Chem., Intl. Engl. Ed.* **1997**, *36*, 1078.

(15) Korgel, B. A.; Fritzmaurice, D. *Phys. Rev. Lett.* **1998**, *80*, 3531.

(16) Korgel, B. A.; Fullam, S.; Connolly, S.; Fitzmaurice, D. *J. Phys. Chem. B* **1998**, *102*, 8379.

(17) Markovich, G.; Collier, C. P.; Hendricks, S. E.; Ramacle, F.; Levine, R. D.; Heath, J. R. *Acc. Chem. Res.* **1999**, *32*, 415.

(18) Teranishi, T.; Miyake, M. *Chem. Mater.* **1998**, *10*, 594.

(19) Teranishi, T.; Hori, H.; Miyake, M. *J. Phys. Chem. B* **1997**, *101*, 5774.

(20) Schmidt, G.; Harns, M.; Malm, J. O.; Bovin, J. O.; Ruitentecik, J. V.; Zandbergen, H. W.; Fu, T. *J. Am. Chem. Soc.* **1993**, *115*, 2046.

(21) Porta, F.; Ragaini, F.; Cenini, S. *Gazz. Chem. Ital.* **1992**, *122*, 361.

(22) Wang, Z. L. *Adv. Mater.* **1998**, *10*, 13.

(23) Fink, J.; Kiely, C. J.; Bethell, D.; Schiffrin, D. J. *Chem. Mater.* **1998**, *10*, 922.

(24) Schmidt, G.; Bäumle, M.; and Beyer. N. *Angew. Chem., Int. Ed. Engl.* **2000**, *1*, 39.

(25) Speedy, R. J. *J. Phys. Condes. Mater.* **1998**, *10*, 4185.

(26) Bargeman, D.; Vader, F. V. V. *J. Electroanal. Chem.* **1972**, *37*, 45.

(27) Israelachvili, J. N. *Intermolecular and surface forces*; Academic Press: London, 1992.